Original Article

J Korean Soc Radiol 2024;85(2):394-408
https://doi.org/10.3348/jksr.2023.0011
eISSN 2951-0805

JOURNAL of THE KOREAN SOCIETY of RADIOLOGY

Predictions of PD-L1 Expression Based on CT Imaging Features in Lung Squamous Cell Carcinoma

편평세포폐암에서 CT 영상 소견을 이용한 PD-L1 발현 예측

Seong Hee Yeo, MD[1], Hyun Jung Yoon, MD[1]*, Injoong Kim, MD[1], Yeo Jin Kim, MD[1], Young Lee, MS[2], Yoon Ki Cha, MD[3], So Hyeon Bak, MD[4]

[1]Department of Radiology, Veterans Health Service Medical Center, Seoul, Korea
[2]Veterans Medical Research Institute, Veterans Health Service Medical Center, Seoul, Korea
[3]Department of Radiology, Samsung Medical Center, Sungkyunkwan University School of Medicine, Seoul, Korea
[4]Department of Radiology, Asan Medical Center, University of Ulsan College of Medicine, Seoul, Korea

Received January 25, 2023
Revised June 21, 2023
Accepted August 10, 2023

***Corresponding author**
Hyun Jung Yoon, MD
Department of Radiology, Veterans Health Service Medical Center,
53 Jinhwangdo-ro 61-gil, Gangdong-gu, Seoul 05368, Korea.

Tel 82-2-2225-3967
Fax 82-2-2225-1433
E-mail pinnari@hanmail.net

Purpose To develop models to predict programmed death ligand 1 (PD-L1) expression in pulmonary squamous cell carcinoma (SCC) using CT.

Materials and Methods A total of 97 patients diagnosed with SCC who underwent PD-L1 expression assay were included in this study. We performed a CT analysis of the tumors using pretreatment CT images. Multiple logistic regression models were constructed to predict PD-L1 positivity in the total patient group and in the 40 advanced-stage (≥ stage IIIB) patients. The area under the receiver operating characteristic curve (AUC) was calculated for each model.

Results For the total patient group, the AUC of the 'total significant features model' (tumor stage, tumor size, pleural nodularity, and lung metastasis) was 0.652, and that of the 'selected feature model' (pleural nodularity) was 0.556. For advanced-stage patients, the AUC of the 'selected feature model' (tumor size, pleural nodularity, pulmonary oligometastases, and absence of interstitial lung disease) was 0.897. Among these factors, pleural nodularity and pulmonary oligometastases had the highest odds ratios (8.78 and 16.35, respectively).

Conclusion Our model could predict PD-L1 expression in patients with lung SCC, and pleural nodularity and pulmonary oligometastases were notable predictive CT features of PD-L1.

Index terms Lung Squamous Cell Carcinoma; Immunotherapy; Programmed Death Ligand 1; Computed Tomography

INTRODUCTION

Lung cancer is the leading cause of cancer-related deaths worldwide, and squamous cell carcinoma (SCC) of the lungs accounts for 30% of all lung cancer cases (1, 2). In cases of pulmonary adenocarcinoma (ADC), the identification of epidermal growth factor receptor *(EGFR)* mutations and anaplastic lymphoma kinase *(ALK)* rearrangements has led to the development of drugs that specifically target these proteins; thus, more treatment options are available. However, unlike in ADC, genetic mutations are less prevalent in SCC, and targeted therapies for SCC have not been established (3, 4). Immune checkpoint inhibitors that target programmed cell death protein 1 (PD-1) or programmed death ligand 1 (PD-L1) have recently been discovered (5). This immune checkpoint inhibitor promotes T cell activity and inhibits the PD-1/PD-L1 pathway by directly binding to PD-1 or its ligand (PD-L1), consequently leading to the destruction of tumor cells (6-9). Currently, this immune checkpoint inhibitor is gaining attention as a novel immunotherapy tool for the treatment of both ADC and SCC because it demonstrates superior treatment efficacy and improves prognosis compared with existing chemotherapeutic agents (4, 8, 10, 11). Consequently, measurement of PD-L1 expression in tumors has become very important for treatment planning, as it can be used to predict the response to immune checkpoint inhibitors (12, 13). Therefore, there is an ongoing effort to identify biomarkers of PD-L1 expression in pulmonary SCC and ADC (14-18).

Currently, PD-L1 expression can only be evaluated in specimens obtained via biopsy or surgical resection (19, 20). However, specimens obtained using these methods often do not contain sufficient tissue for PD-L1 staining. Furthermore, invasive sampling methods for detecting PD-L1 expression may not be suitable for patients with advanced disease because of the associated intrinsic limitations and risks. Therefore, the development of noninvasive techniques for predicting PD-L1 expression is gaining importance (21). Several studies have demonstrated correlations between CT imaging features and PD-L1 expression in pulmonary ADC. PD-L1 expression has been found to be associated with the pathological invasiveness of ADCs and CT features, suggesting the possibility of using imaging features to predict PD-L1 expression status (10, 14, 22). As such, PD-L1 expression may be correlated with certain CT imaging features in pulmonary SCC, and CT findings may aid in identifying patients suitable for immune checkpoint inhibitor treatment, even when insufficient quantities of tissue have been obtained using invasive techniques (10, 14). Prediction of PD-L1 expression based on CT imaging features of SCC, which are relatively weakly associated with *EGFR* and *ALK*, is particularly valuable (9, 23, 24). However, few studies have investigated the association between SCC and CT findings.

Thus, in this study, we aimed to identify the associations between clinicopathological factors, CT findings, and PD-L1 expression in SCC based on biopsy or surgical findings, develop models to predict PD-L1 expression based on CT imaging features, and evaluate their performance in predicting PD-L1 positivity.

JOURNAL of THE KOREAN SOCIETY of RADIOLOGY

MATERIALS AND METHODS

PATIENTS

Our Institutional Review Board approved this retrospective study and waived the requirement for informed consent (IRB No. 2021-01-024). We initially identified 110 patients diagnosed with pulmonary SCC between January 2015 and 2020 whose pathological reports included a tumor proportion score (TPS) based on a PD-L1 expression assay. Among the 112 patients, 13 were excluded for the following reasons: 1) recurrent tumors (n = 6), 2) presence of other malignancies (n = 1), 3) multiple primary lung cancers (n = 5), and 4) unavailability of preoperative CT images (n = 1). A total of 97 patients who were diagnosed with pulmonary SCC on pathological examination and whose tissue samples were subjected to immunohistochemical analysis to assess PD-L1 expression were included in the study. The patient selection process is illustrated in Fig. 1. Clinicopathological data were collected from electronic medical records at the time of the diagnostic work-up. The patients' sex and age, method used to obtain tissue samples and site, TNM stage according to the eighth edition of the International Association for the Study of Lung Cancer (IASLC) guidelines (25), presence of extrathoracic metastases, *EGFR* mutation status, and tumor differentiation were recorded.

CT IMAGE ACQUISITION

For all patients, contrast-enhanced chest CT scans of the thoracic inlet to the subcostal plane were performed before pathological confirmation using one of the following multidetector row scanners: Revolution Discovery CT, Discovery CT750 HD (GE Healthcare, Milwaukee, WI, USA), or SOMATOM® Definition Flash (Siemens Medical Solutions, Forchheim, Germany). Details of the scanning parameters were as follows: detector collimation, 1.25 or 0.625 mm; field of view, 34–36 cm; beam pitch, 0.992–1.531; beam width, 80 mm; gantry speed, 0.35 seconds per rotation; 120 kVp; 80–650 mA; reconstruction interval, 2 mm; and matrix, 512 × 512 mm. A bolus of 50–90 mL (1.5 mL/kg body weight) of Optisure or Bonorex was injected intravenously at a flow rate of 3 mL/s for enhanced imaging using an automated bolus-tracking technique. Axial and coronal images were reconstructed with soft tissue and bone kernels, and a slice thickness of 2–3 mm.

EVALUATION OF CT IMAGING FEATURES

The CT images of the patients were analyzed independently by two thoracic radiologists (with 3 and 12 years of experience in chest CT imaging, respectively) who were blinded to the clinical information and histological findings. When there was a disagreement between the two readers regarding imaging features, the final decisions were determined by consensus. Axial and coronal views of the CT images were analyzed using mediastinal (width, 400 Hounsfield units [HU]; level, 20 HU) and lung (width, 1500 HU; level, -700) window settings. The following CT imaging features were evaluated: 1) size (maximal diameter), lesion type (nodule or mass, endo/peribronchial lesion, mixed), distribution (central or peripheral), location, tumor margin (smooth, spiculated, or lobulated) and shape (round, lobular, or irregular) of the primary mass, 2) internal characteristics of the tumor (presence of calcification, cavitation or necrosis, pre/post enhanced HU and ΔHU), 3) associated findings (pleural retraction

or invasion, presence of pleural effusion, pleural nodularity, presence of lung metastasis, and lymph node [N] stage), and 4) external characteristics of the tumor (emphysema and interstitial lung disease).

Radiologists also analyzed CT features, such as the presence of lung metastasis and the pattern of lung metastasis if present (oligometastases [defined as 1–5 metastases in the lung], multiple, or lymphangitic) for advanced-stage pulmonary SCC (≥ stage IIIB according to the TNM classification according to the eighth edition of the IASLC guidelines) (25).

ANALYSIS OF PD-L1 EXPRESSION

PD-L1 expression in histopathological specimens was determined using a PD-L1 22C3 pharmDx antibody (Dako North America Inc., Carpinteria, CA, USA) or a Ventana PD-L1 SP263 antibody (Ventana Medical Systems, Tucson, AZ, USA) as a companion diagnosis. Tumor cells with complete circumferential or partial cell membrane staining were defined as PD-L1-positive cells. Cytoplasmic staining and tumor-associated immune cells (such as macrophages) were excluded from scoring. Finally, TPS was calculated as the percentage of PD-L1-positive tumor cells relative to the total number of tumor cells. We defined tumor tissue specimens as "PD-L1-expression-positive" when 5% or more viable tumor cells exhibited membrane staining at any intensity (TPS ≥ 5%) (6, 12, 26-30). The 97 enrolled patients were divided into two groups according to PD-L1 expression: a "PD-L1-positive" group and a "PD-L1-negative" group. Additionally, 40 advanced-stage patients among the 97 patients were divided into two groups according to PD-L1 expression. The median (interquartile range [IQR]) time interval between the CT acquisition and tissue sampling for analysis of PD-L1 expression was 16 days (9.5–28.5).

DATA MANAGEMENT AND STATISTICAL ANALYSES

All statistical analyses were performed using R software, version 4.1.2 (R Foundation for Statistical Computing, Vienna, Austria; http://www.R-project.org). The development of predictive models for PD-L1 expression was based on data from 97 patients with lung SCC and 40 advanced-stage patients (Fig. 1). Categorical variables are presented as numbers and percentages. Continuous variables are presented as medians (IQR). Clinicopathological and CT imaging features of the PD-L1-positive and -negative groups were compared using the chi-square test or Fisher's exact test for categorical variables and the independent *t*-test (variables with normality) or Mann–Whitney U test (variables without normality) for continuous variables. Firth's logistic regression analysis was performed to determine the association between PD-L1 expression and clinicopathological and CT features to overcome the issues of separation (31, 32). To develop a predictive model of PD-L1 expression, features with $p < 0.2$ in univariate analysis and/or clinical significance based on our clinical experience were selected as 'total significant features' for PD-L1 expression status. We calculated the generalized variance inflation factor (GVIF) to detect multicollinearity. To make the GVIFs comparable across dimensions, we also calculated the $GVIF^{1/2 \times df}$, where df is the degrees of freedom of the variable. A $GVIF^{1/2 \times df}$ higher than 2 was regarded as a sign of multicollinearity, and no variables were greater than 2. All total significant features were used in the multiple logistic regression analyses. For final feature selection, multiple regression was performed using the total significant features through a backward process until the smallest Akaike information criterion

JOURNAL of THE KOREAN SOCIETY of RADIOLOGY

Fig. 1. Development of a predictive model of PD-L1 expression in pulmonary squamous cell carcinoma.

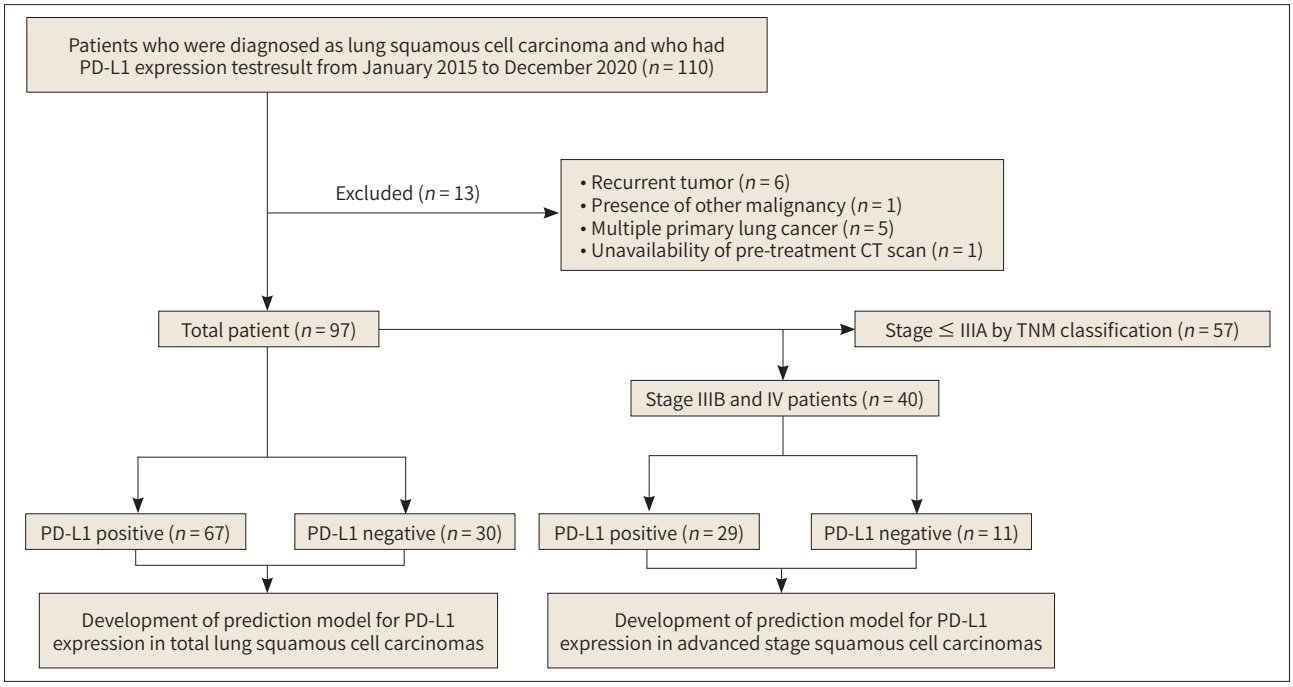

PD-L1 = programmed death ligand 1

(AIC) value was reached ('selected features') (33-35). Receiver operating characteristic curves were generated, and area under the receiver operating characteristic curve (AUC) were calculated to evaluate the predictive performance of the models.

We performed similar statistical analyses to evaluate the clinicopathological and CT features according to PD-L1 expression and developed a predictive model for advanced-stage pulmonary SCCs (≥ stage IIIB), focusing on associated CT features (presence of pleural effusion, pleural nodularity, presence of lung metastasis, pattern of lung metastasis if present, and N stage).

RESULTS

Among the 97 patients, 67 (69.1%) were PD-L1-positive and 30 (30.9%) were PD-L1-negative. Surgery was performed in 31 patients (32.0%), percutaneous transthoracic cutting needle biopsy in 27 (27.8%), and transbronchial lung biopsy with or without endobronchial ultrasound-guided transbronchial needle aspiration in 39 (40.2%). All 97 samples were lung tissues. Among the 40 advanced-stage patients, 29 (72.5%) were PD-L1-positive and 11 (27.5%) were PD-L1-negative. The demographic information and tumor characteristics of the total and advanced-stage patients are listed in Tables 1 and 2, respectively.

ASSOCIATIONS OF CLINICOPATHOLOGICAL AND CT FEATURES WITH PD-L1 EXPRESSION IN THE STUDY PATIENT POPULATION

Comparisons of clinicopathological and CT features according to PD-L1 expression and the results of univariate analysis in the 97 patients included in the study are presented in Table 1.

Table 1. Comparison of Clinicopathological and CT Features according to PD-L1 Expression and Univariate Analysis in Total Patients

	Total (*n* = 97)	Negative (*n* = 30)	Positive (*n* = 67)	*p*-Value*	Univariate	
					OR (95% CI)	*p*-Value
Age, median (IQR), years	73.0 (71.0–77.0)	73.5 (71.0–80.0)	73.0 (71.0–76.5)	0.359	0.97 (0.89, 1.04)	0.360
Sex, male	97 (100.0)	30 (100.0)	67 (100.0)			
Tissue obtain method				0.387		
Surgery	31 (32.0)	11 (36.7)	20 (29.9)		Reference	
PCNB	27 (27.8)	10 (33.3)	17 (25.4)		0.93 (0.32, 2.73)	0.902
TBLB ± EBUS-TBNA	39 (40.2)	9 (30.0)	30 (44.8)		1.80 (0.64, 5.10)	0.268
Tissue sample site						
Lung	97 (100.0)	30 (100.0)	67 (100.0)			
Tumor stage				0.635		
I	20 (20.6)	8 (26.7)	12 (17.9)		Reference	
II	18 (18.6)	5 (16.7)	13 (19.4)		1.67 (0.43, 6.47)	0.459
III	26 (26.8)	9 (30.0)	17 (25.4)		1.25 (0.38, 4.17)	0.713
IV	33 (34.0)	8 (26.7)	25 (37.3)		2.04 (0.62, 6.71)	0.241
Extrathoracic metastasis, yes	11 (11.3)	4 (13.3)	7 (10.4)	0.734	0.73 (0.20, 2.69)	0.636
EGFR mutation, yes	8 (9.4)	3 (11.5)	5 (8.5)	0.696	0.68 (0.15, 3.04)	0.612
Tumor differentiation				0.063		
Well	2 (2.6)	0 (0.0)	2 (3.9)		Reference	
Moderate	56 (73.7)	15 (60.0)	41 (80.4)		Inf (Inf-Inf)	
Poor	18 (23.7)	10 (40.0)	8 (15.7)		0 (0-0)	
Primary tumor size (mm), median (IQR)	46.0 (29.0–60.0)	32.0 (26.0–63.0)	48 (30.5–60.0)	0.142	1.02 (0.99, 1.04)	0.160
Lesion type				0.567		
Nodule or mass	68 (70.1)	19 (63.3)	49 (73.1)		Reference	
Endo/peribronchial lesion	10 (10.3)	4 (13.3)	6 (9.0)		0.57 (0.15, 2.23)	0.419
Mixed	19 (19.6)	7 (23.3)	12 (17.9)		0.66 (0.23, 1.91)	0.440
Distribution				0.774		
Central	49 (50.5)	14 (46.7)	35 (52.2)		Reference	
Peripheral	48 (49.5)	16 (53.3)	32 (47.8)		0.80 (0.34, 1.90)	0.620
Location				0.04		
Right upper lobe	29 (29.9)	10 (33.3)	19 (28.4)		Reference	
Right middle lobe	6 (6.2)	0 (0.0)	6 (9.0)		7.00 (0.29, 171.60)	0.233
Right lower lobe	28 (28.9)	6 (20.0)	22 (32.8)		1.86 (0.58, 6.01)	0.297
Left upper lobe	15 (15.5)	9 (30.0)	6 (9.0)		0.37 (0.10, 1.33)	0.127
Left lower lobe	14 (14.4)	3 (10.0)	11 (16.4)		1.77 (0.41, 7.58)	0.442
Right central bronchi	3 (3.1)	2 (6.7)	1 (1.5)		0.32 (0.03, 3.78)	0.368
Left central bronchi	2 (2.1)	0 (0.0)	2 (3.0)		2.69 (0.06, 119.90)	0.609
Margin				1		
Smooth	1 (1.2)	0 (0.0)	1 (1.8)		Reference	
Spiculated or lobulated	80 (98.8)	24 (100.0)	56 (98.2)		0 (0-0)	
Shape				0.978		
Round	43 (44.8)	14 (46.7)	29 (43.9)		Reference	
Lobular or irregular	53 (55.2)	16 (53.3)	37 (56.1)		1.12 (0.47, 2.65)	0.802

Table 1. Comparison of Clinicopathological and CT Features according to PD-L1 Expression and Univariate Analysis in Total Patients (Continued)

	Total (*n* = 97)	Negative (*n* = 30)	Positive (*n* = 67)	*p*-Value*	Univariate	
					OR (95% CI)	*p*-Value
Calcification, yes	0 (0)	0 (0)	0 (0)			
Cavity or profuse necrosis, yes	38 (39.2)	10 (33.3)	28 (41.8)	0.573	1.41 (0.57, 3.45)	0.451
Pre enhanced HU, median (IQR)	35.2 (26.9–40.4)	36.3 (24.4–40.1)	35.1 (27.2–41.1)	0.682	1.01 (0.97, 1.05)	0.679
Post enhanced HU, median (IQR)	63.9 (55.4–75.5)	70.8 (56.8–78.3)	62.4 (55.2–73.4)	0.781	1.00 (0.97, 1.02)	0.781
ΔHU, median (IQR)	29.8 (20.6–39.7)	32.5 (25.6–42.6)	27.8 (19.9–38.6)	0.534	0.99 (0.96, 1.02)	0.530
Pleural retraction or invasion, yes	45 (46.4)	12 (40.0)	33 (49.3)	0.532	1.44 (0.60, 3.43)	0.414
Pleural effusion, yes	20 (20.6)	6 (20.0)	14 (20.9)	1	1.02 (0.35, 2.96)	0.969
Pleural nodularity, yes	14 (14.4)	2 (6.7)	12 (17.9)	0.214	2.57 (0.59, 11.26)	0.211
Lung metastasis, yes	16 (16.5)	3 (10.0)	13 (19.4)	0.376	1.95 (0.53, 7.12)	0.314
N stage				0.918		
N0	48 (49.5)	15 (50.0)	33 (49.3)		Reference	
N1	16 (16.5)	6 (20.0)	10 (14.9)		0.75 (0.23, 2.43)	0.628
N2	21 (21.6)	6 (20.0)	15 (22.4)		1.10 (0.36, 3.37)	0.863
N3	12 (12.4)	3 (10.0)	9 (13.4)		1.26 (0.31, 5.16)	0.752
Emphysema, yes	37 (38.5)	9 (31.0)	28 (41.8)	0.444	1.56 (0.62, 3.90)	0.345
Interstitial lung disease, yes	13 (13.4)	5 (16.7)	8 (11.9)	0.533	0.66 (0.20, 2.21)	0.503

Unless otherwise indicated, data in parentheses are percentages.
**p*-values obtained by chi-square test or Fisher's exact test for categorical variables and independent *t*-test or Mann-Whitney U test for continuous variables.
CI = confidence interval, EBUS-TBNA = endobronchial ultrasound guided transbronchial needle aspiration, *EGFR* = epidermal growth factor receptor, HU = Hounsfield unit, Inf = infinite, IQR = interquartile range, OR = odds ratio, PCNB = percutaneous transthoracic cutting needle biopsy, PD-L1 = programmed death ligand 1, TBLB = transbronchial lung biopsy

Based on the feature selection requirements in the univariate analyses for the prediction of PD-L1 expression, higher tumor stage (stage IV, $p = 0.241$), larger primary tumor size ($p = 0.160$), presence of pleural nodularity ($p = 0.211$), and presence of lung metastases ($p = 0.314$) were candidates for multivariate analysis. Although the *p*-values of higher tumor stage, presence of pleural nodularity, and presence of lung metastases were not < 0.2, we selected these variables because they could reflect the invasiveness of the tumor with PD-L1 expression, which has been noted in previous studies (10, 14, 22). The results of the multiple logistic regression analyses are presented in Table 3. In multivariate analyses of total significant features, the odds ratios (OR) for the presence of pleural nodularity and lung metastasis were 3.01 and 2.30, respectively. When we performed a multiple regression analysis using the total significant features through a backward process until the smallest AIC value was obtained, only pleural nodularity was selected ($p = 0.211$, OR = 2.57).

ASSOCIATIONS OF CLINICOPATHOLOGICAL AND CT FEATURES WITH PD-L1 EXPRESSION IN ADVANCED-STAGE PATIENTS

Comparisons of clinicopathological and CT features according to PD-L1 expression and the results of univariate analysis in 40 patients with advanced-stage disease, defined as stage IIIB or higher, are presented in Table 2. According to our feature selection requirements, in the

Table 2. Comparison of Clinicopathological and CT Features according to PD-L1 Expression and Univariate Analysis in Advanced-Stage Patients

	Total (*n* = 40)	Negative (*n* = 11)	Positive (*n* = 29)	*p*-Value*	Univariate	
					OR (95% CI)	*p*-Value
Age, median (IQR), years	74.0 (71.0–77.0)	73.0 (71.5–82.0)	74.0 (70.0–76.0)	0.501	0.96 (0.86, 1.08)	0.511
Sex, male	40 (100.0)	11 (100.0)	29 (100.0)			
Tissue sample method				0.868		
Surgery	3 (7.5)	1 (9.1)	2 (6.9)		Reference	
PCNB	15 (37.5)	5 (45.5)	10 (34.5)		1.15 (0.09, 14.95)	0.917
TBLB ± EBUS-TBNA	22 (55.0)	5 (45.5)	17 (58.6)		1.91 (0.15, 24.07)	0.617
Tissue obtain site				1		
Lung	40 (97.6)	11 (100.0)	29 (96.7)			
Tumor stage				0.369		
IIIB	7 (17.5)	3 (27.3)	4 (13.8)		Reference	
IV	33 (82.5)	8 (72.7)	25 (86.2)		2.33 (0.43, 12.63)	0.325
Extrathoracic metastasis, yes	11 (27.5)	4 (36.4)	7 (24.1)	0.445	0.56 (0.13, 2.45)	0.437
EGFR mutation, yes	1 (2.8)	1 (9.1)	0 (0.0)	0.306	0 (0–0)	
Tumor differentiation				0.345		
Well	0 (0.0)	0 (0.0)	0 (0.0)			
Moderate	23 (76.7)	5 (62.5)	18 (81.8)		Reference	
Poor	7 (23.3)	3 (37.5)	4 (18.2)		0.38 (0.06, 2.27)	0.290
Primary tumor size (mm), median (IQR)	59.5 (49.5–70.4)	52.0 (42.0–68.4)	60.0 (52.0–68.0)	0.691	1.02 (0.98, 1.07)	0.236
Lesion type				1		
Nodule or mass	30 (75.0)	9 (81.8)	21 (72.4)		Reference	
Endo/peribronchial lesion	1 (2.5)	0 (0.0)	1 (3.4)		Inf (Inf-Inf)	
Mixed	9 (22.5)	2 (18.2)	7 (24.1)		1.33 (0.24, 7.23)	0.745
Distribution				0.366		
Central	21 (52.5)	4 (36.4)	17 (58.6)		Reference	
Peripheral	19 (47.5)	7 (63.6)	12 (41.4)		0.43 (0.10, 1.75)	0.239
Pleural effusion, yes	16 (40.0)	3 (27.3)	13 (44.8)	0.473	1.99 (0.45, 8.70)	0.362
Pleural nodularity, yes	12 (30.0)	2 (18.2)	10 (34.5)	0.451	2.05 (0.40, 10.53)	0.392
Lung metastasis, yes	13 (32.5)	2 (18.2)	11 (37.9)	0.286	2.36 (0.46, 12.03)	0.301
Lung metastasis				0.19		
No	27 (67.5)	9 (81.8)	18 (62.1)		References	
Oligo	10 (25.0)	1 (9.1)	9 (31.0)		3.25 (0.45, 23.41)	0.242
Multiple	1 (2.5)	1 (9.1)	0 (0.0)		0.17 (0.00, 16.96)	0.452
Lymphangitic	2 (5.0)	0 (0.0)	2 (6.9)		2.57 (0.06, 115.14)	0.627
N stage				0.763		
N0	10 (25.0)	4 (36.4)	6 (20.7)		Reference	
N1	7 (17.5)	2 (18.2)	5 (17.2)		1.52 (0.20, 11.66)	0.685
N2	11 (27.5)	2 (18.2)	9 (31.0)		2.63 (0.38, 18.03)	0.325
N3	12 (30.0)	3 (27.3)	9 (31.0)		1.88 (0.31, 11.29)	0.491
Emphysema, yes	13(33.3)	3(30.0)	10(34.5)	1	1.15 (0.25, 5.28)	0.854
Interstitial lung disease, yes	6 (15.0)	4 (36.4)	2 (6.9)	0.039	0.15 (0.02, 0.97)	0.047

Unless otherwise indicated, data in parentheses are percentages.

**p*-values obtained by chi-square test or Fisher's exact test for categorical variables and independent *t*-test or Mann-Whitney U test for continuous variables.

CI = confidence interval, EBUS-TBNA = endobronchial ultrasound guided transbronchial needle aspiration, *EGFR* = epidermal growth factor receptor, HU = Hounsfield unit, Inf = infinite, IQR = interquartile range, OR = odds ratio, PCNB = percutaneous transthoracic cutting needle biopsy, PD-L1 = programmed death ligand 1, TBLB = transbronchial lung biopsy

Table 3. Multiple Logistic Regression Models for the Prediction of PD-L1 Positivity in Total Patients

	Odds Ratio	95% Confidence Interval	*p*-Value
Total significant features			
Tumor stage			
I		Reference	
II	1.23	0.29–5.23	0.776
III	0.91	0.24–3.45	0.885
IV	0.66	0.12–3.69	0.638
Primary tumor size	1.01	0.99–1.04	0.288
Pleural nodularity	3.01	0.55–16.52	0.206
Lung metastasis	2.30	0.50–10.49	0.282
Selected feature			
Pleural nodularity	2.57	0.59–11.25	0.211

PD-L1 = programmed death ligand 1

Table 4. Multiple Logistic Regression Models for the Prediction of PD-L1 Positivity in Advanced-Stage Patients

	OR	95% CI	*p*-Value		OR	95% CI	*p*-Value
Model 1 (total significant features)				Model 1* (selected features)			
Primary tumor size	1.06	1.00–1.12	0.159	Primary tumor size	1.06	1.00–1.12	0.060
Distribution	0.43	0.05–4.03	0.461				
Pleural effusion	1.41	0.14–14.59	0.773				
Pleural nodularity	6.75	0.46–99.70	0.165	Pleural nodularity	8.78	0.78–98.95	0.079
Lung metastasis				Lung metastasis			
No				No			
Oligo	17.69	1.03–304.19	0.048	Oligo	16.35	1.10–243.27	0.043
Multiple	0.14	0.00–15.97	0.411	Multiple	0.18	0.00–18.91	0.469
Lymphangitic	2.59	0.04–156.23	0.650	Lymphangitic	2.55	0.05–119.76	0.634
Interstitial lung disease	0.17	0.02–1.87	0.147	Interstitial lung disease	0.10	0.01–0.95	0.045
Model 2 (total significant features)				Model 2* (selected features)			
Primary tumor size	1.04	0.99–1.10	0.116	Primary tumor size	1.04	0.99–1.10	0.094
Distribution	0.82	0.12–5.72	0.838				
Pleural effusion	1.14	0.16–8.39	0.896				
Pleural nodularity	5.62	0.50–63.25	0.162	Pleural nodularity	6.86	0.75–62.31	0.087
Lung metastasis	5.54	0.78–39.48	0.088	Lung metastasis	6.06	0.82–44.95	0.078
Interstitial lung disease	0.19	0.02–1.86	0.155	Interstitial lung disease	0.15	0.02–1.14	0.067

CI = confidence interval, OR = odds ratio, PD-L1 = programmed death ligand 1

univariate analyses for prediction of PD-L1 expression, tumor size ($p = 0.236$), distribution ($p = 0.239$), pleural effusion ($p = 0.362$), pleural nodularity ($p = 0.392$), presence of lung metastasis ($p = 0.301$), pulmonary oligometastases ($p = 0.242$), and presence of interstitial lung disease ($p = 0.047$) were candidates for multivariate analyses. The *p*-values of tumor size, pleural effusion, pleural nodularity, presence of lung metastasis, and pulmonary oligometastases were not < 0.2, but they were selected as significant features because they could reflect the invasiveness of the tumor with PD-L1 expression. Distribution (central or peripheral) and pulmonary oligometas-

tases were also selected because tumors expressing PD-L1 tend to be centrally located and show pulmonary oligometastases on CT.

The results of the multiple logistic regression analysis are presented in Table 4. Two separate models were developed for the multivariate analysis of lung metastases. Model 1 categorized lung metastasis type into "oligometastases, multiple metastases, and lymphangitic metastases," while Model 2 simply categorized the presence of lung metastasis as "yes or no." When we performed multiple regression analysis using the total significant features through a backward process until the smallest AIC value was obtained, larger primary tumor size (p = 0.060, OR = 1.06), presence of pleural nodularity (p = 0.079, OR = 8.78), pulmonary oligometastases (p = 0.043, OR = 16.35), and absence of interstitial lung disease (p = 0.045, OR = 0.10) were selected for Model 1 (Fig. 2), while larger primary tumor size (p = 0.094, OR = 1.04), presence of pleural nodularity (p = 0.087, OR = 6.86), presence of lung metastases (p = 0.078, OR = 6.06), and absence of interstitial lung disease (p = 0.067, OR = 0.15) were selected for Model 2.

PREDICTIVE PERFORMANCE FOR MODEL PD-L1 POSITIVITY

For the 97 study patients, the AUC value of the 'total significant features model' (tumor stage, primary tumor size, pleural nodularity and lung metastasis) was 0.65 and the AUC value of the 'selected features model' (pleural nodularity) was 0.556 (Fig. 3A).

For the 40 advanced-stage patients, the AUC of the total significant features model (primary

Fig. 2. The representative CT images of a 74-year-old male show pulmonary squamous cell carcinoma positive for PD-L1 expression.
A. A mediastinal setting image of a contrast-enhanced CT scan shows a central primary lung cancer in the left upper lobe (white arrow) and pleural nodularity (black arrows) with pleural effusion (arrowhead) in the ipsilateral hemithorax.
B. A lung setting image shows a metastatic nodule in the right lower lobe (arrow).
PD-L1 = programmed death ligand 1

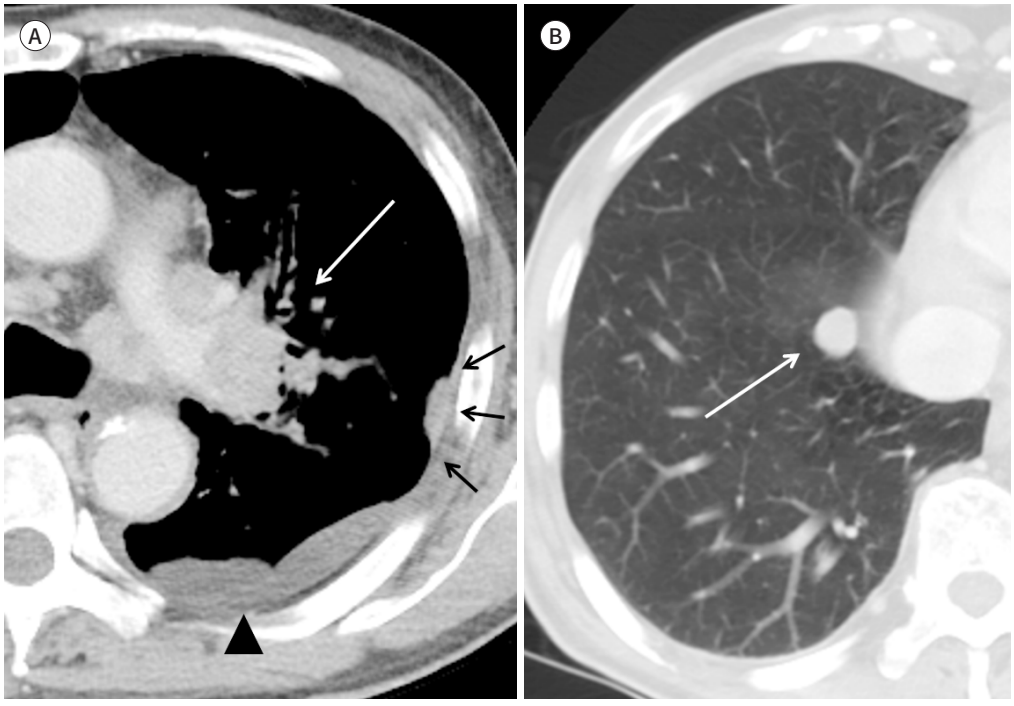

Fig. 3. Receiver operator characteristic curves of the predictive models developed for the total study patient population (A), Model 1 (B), and Model 2 (C) of the advanced-stage patients.
AUC = areas under the curve

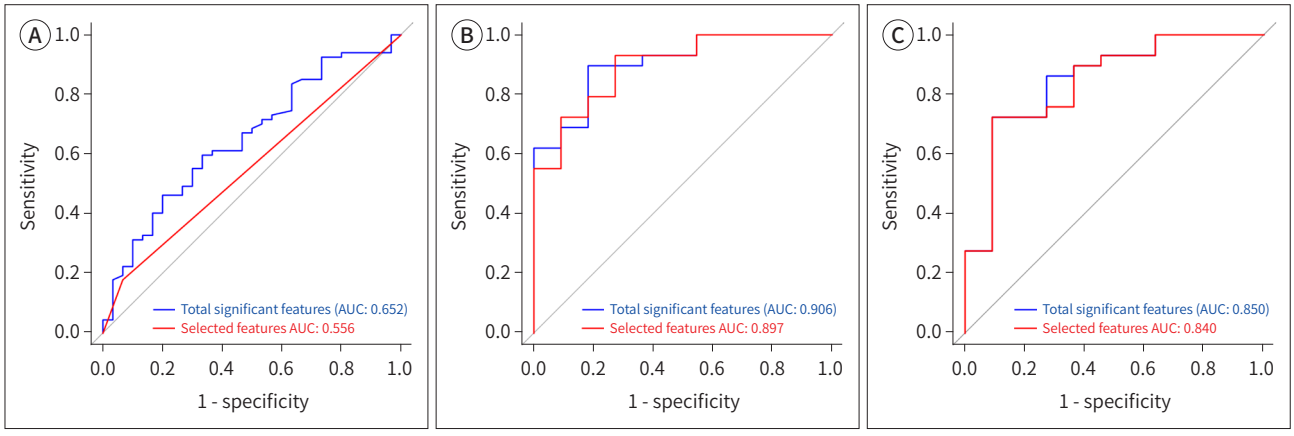

tumor size, distribution, pleural effusion, pleural nodularity, pulmonary oligometastases, and interstitial lung disease) and the selected features model (primary tumor size, pleural nodularity, pulmonary oligometastases, and interstitial lung disease) in Model 1 were 0.906 and 0.897, respectively, whereas those for the total significant features model (primary tumor size, distribution, pleural effusion, pleural nodularity, presence of lung metastasis, and interstitial lung disease) and the selected features model (primary tumor size, pleural nodularity, presence of lung metastasis, and interstitial lung disease) in Model 2 were 0.850 and 0.840, respectively (Fig. 3B, C).

Demographic information and a comparison of clinicopathological and CT features according to PD-L1 expression in the 29 patients who underwent surgical resection without neoadjuvant chemotherapy are presented in Supplementary Table 1.

DISCUSSION

Our study demonstrated that significant CT features were associated with PD-L1 expression in pulmonary SCC tissue specimens, and we were able to develop predictive models. For the total study patient population, the AUC of the total significant features model (tumor stage, primary tumor size, presence of pleural nodularity, and lung metastasis) and the selected features model (pleural nodularity) were 0.652 and 0.556, respectively. Among the selected features, the OR for pleural nodularity was 2.57. For advanced-stage patients, the AUC of the total significant features model (primary tumor size, distribution, presence of pleural effusion, pleural nodularity, pulmonary oligometastases, and interstitial lung disease) and the selected feature model (primary tumor size, presence of pleural nodularity, pulmonary oligometastases, and absence of interstitial lung disease) in Model 1 were 0.906 and 0897, respectively. Among the selected features, the ORs for pleural nodularity and pulmonary oligometastases were high at 8.78 and 16.35, respectively. Based on these results, we found that pleural nodularity and pulmonary oligometastases are valuable predictive CT features in advanced-stage patients.

In our study, we selected CT features, including higher tumor stage, primary tumor size,

presence of pleural nodularity, and lung metastasis, found in the study patient population through univariate analyses and used them as input variables for multivariate analyses based on clinical significance and *p*-value. Although the *p*-values of these features were not very low in the univariate and multivariate analyses, comparative analyses of clinicopathological and CT features according to PD-L1 expression showed a tendency toward a higher tumor stage, larger tumor size, presence of pleural nodularity, and pulmonary metastases. In addition, the differentiation performance of the models obtained by combining these factors was obtained through multivariate regression using a backward process until the smallest AIC value was sufficient to predict PD-L1 expression. However, because a significant number of the study patients had resectable tumors, they showed relatively low statistical power for application as prediction models.

Therefore, we developed separate predictive models for advanced-stage patients with significant CT features, using the same method as that used for the total patient group. Compared with the total patient group, the AUCs of total significant features and selected features in Model 1 for advanced-stage patients were 0.906 and 0.897, respectively, indicating a high predictive value of the models of PD-L1 expression. Among the selected features of Model 1, pulmonary oligometastases had a very high OR of 16.35, and the presence of pleural nodularities also had a high ORs (8.78 in Model 1 and 6.86 in Model 2). These results are novel and have not been reported previously. Several previous studies have assessed radiological predictive markers of PD-L1 expression, but these were limited to pulmonary ADC (10, 14, 22). Further studies are needed to validate whether targeted PD-L1 immunotherapy is indicated for advanced-stage pulmonary SCC when CT findings show pulmonary oligometastases and pleural nodularity. Nevertheless, we believe our findings and the radiologic phenotype approach described herein are meaningful in terms of building baseline research data for future studies and demonstrated that CT features may have potential utility as predictive markers of PD-L1 expression and advanced-stage SCC in patients who are not suitable for invasive sampling.

This study had several limitations. First, it was conducted retrospectively using patient data from a single center, which may have led to a selection bias. All patients were men over the age of 70 years due to the skewed patient population of the Veterans Hospital. Second, the sample size was small (97 patients and 40 advanced-stage patients); therefore, the statistical power was low, especially for the statistical analysis of 40 advanced-stage patients. Therefore, we consider our findings as preliminary. Third, the statistical results are prone to overfitting owing to the lack of internal and external validation. Fourth, smoking history, which is an important clinical risk factor in patients with lung cancer, was not included as a clinical variable.

In conclusion, our CT-based model was able to predict PD-L1 expression in patients with pulmonary SCC, especially in advanced stages. Among the CT features assessed, primary tumor size, pleural nodularity, pulmonary oligometastases, absence of interstitial lung disease, and presence of pleural nodularities and lung metastases were considered strongly predictive of PD-L1 expression in patients with advanced-stage pulmonary SCC based on high ORs. Furthermore, with respect to metastases, pulmonary oligometastases are a predictive factor for PD-L1 expression in advanced-stage pulmonary SCC. A predictive model based on CT features may facilitate the non-invasive assessment of PD-L1 expression.

Supplementary Materials

The online-only Data Supplement is available with this article at http://doi.org/10.3348/jksr.2023.0011.

Availability of Data and Material

The datasets generated or analyzed during the study are available from the corresponding author on reasonable request.

Author Contributions

Conceptualization, Y.H.J., K.I., B.S.H.; data curation, Y.H.J., C.Y.K.; formal analysis, Y.S.H., Y.H.J., K.I., L.Y.; funding acquisition, Y.H.J.; investigation, K.Y.J., L.Y., C.Y.K., B.S.H.; methodology, all authors; supervision, Y.H.J.; validation, Y.H.J.; writing—original draft, Y.S.H.; and writing—review & editing, Y.S.H., Y.H.J., K.Y.J., L.Y., C.Y.K., B.S.H.

Conflicts of Interest

The authors have no potential conflicts of interest to disclose.

ORCID iDs

Seong Hee Yeo https://orcid.org/0000-0002-5982-7120
Hyun Jung Yoon https://orcid.org/0000-0002-8909-1185
Injoong Kim https://orcid.org/0000-0003-3824-7706
Yeo Jin Kim https://orcid.org/0000-0002-4590-6493
Young Lee https://orcid.org/0000-0003-0178-0187
Yoon Ki Cha https://orcid.org/0000-0002-5960-0719
So Hyeon Bak https://orcid.org/0000-0003-1039-7016

Funding

This study was supported by a VHS Medical Center Research Grant, Republic of Korea (grant number: VHSMC 21007). The funders had no role in study design, data collection, and analysis, decision to publish, or preparation of the manuscript.

REFERENCES

1. Siegel RL, Miller KD, Jemal A. Cancer statistics, 2019. *CA Cancer J Clin* 2019;69:7-34
2. Meza R, Meernik C, Jeon J, Cote ML. Lung cancer incidence trends by gender, race and histology in the United States, 1973-2010. *PLoS One* 2015;10:e0121323
3. Zhang M, Wang D, Sun Q, Pu H, Wang Y, Zhao S, et al. Prognostic significance of PD-L1 expression and 18F-FDG PET/CT in surgical pulmonary squamous cell carcinoma. *Oncotarget* 2017;8:51630-51640
4. Chen RL, Zhou JX, Cao Y, Li SH, Li YH, Jiang M, et al. The efficacy of PD-1/PD-L1 inhibitors in advanced squamous-cell lung cancer: a meta-analysis of 3112 patients. *Immunotherapy* 2019;11:1481-1490
5. Brahmer J, Reckamp KL, Baas P, Crinò L, Eberhardt WE, Poddubskaya E, et al. Nivolumab versus docetaxel in advanced squamous-cell non-small-cell lung cancer. *N Engl J Med* 2015;373:123-135
6. Topalian SL, Hodi FS, Brahmer JR, Gettinger SN, Smith DC, McDermott DF, et al. Safety, activity, and immune correlates of anti-PD-1 antibody in cancer. *N Engl J Med* 2012;366:2443-2454
7. Taube JM, Klein A, Brahmer JR, Xu H, Pan X, Kim JH, et al. Association of PD-1, PD-1 ligands, and other features of the tumor immune microenvironment with response to anti-PD-1 therapy. *Clin Cancer Res* 2014;20:5064-5074
8. Aguiar PN Jr, Santoro IL, Tadokoro H, de Lima Lopes G, Filardi BA, Oliveira P, et al. The role of PD-L1 expression as a predictive biomarker in advanced non-small-cell lung cancer: a network meta-analysis. *Immunotherapy* 2016;8:479-488
9. Wang GX, Guo LQ, Gainor JF, Fintelmann FJ. Immune checkpoint inhibitors in lung cancer: imaging considerations. *AJR Am J Roentgenol* 2017;209:567-575
10. Yoon J, Suh YJ, Han K, Cho H, Lee HJ, Hur J, et al. Utility of CT radiomics for prediction of PD-L1 expression

in advanced lung adenocarcinomas. *Thorac Cancer* 2020;11:993-1004
11. Reck M, Rodríguez-Abreu D, Robinson AG, Hui R, Csőszi T, Fülöp A, et al. Pembrolizumab versus chemotherapy for PD-L1-positive non-small-cell lung cancer. *N Engl J Med* 2016;375:1823-1833
12. McLaughlin J, Han G, Schalper KA, Carvajal-Hausdorf D, Pelekanou V, Rehman J, et al. Quantitative assessment of the heterogeneity of PD-L1 expression in non-small-cell lung cancer. *JAMA Oncol* 2016;2:46-54
13. Nimmagadda S. Quantifying PD-L1 expression to monitor immune checkpoint therapy: opportunities and challenges. *Cancers (Basel)* 2020;12:3173
14. Wu T, Zhou F, Soodeen-Lalloo AK, Yang X, Shen Y, Ding X, et al. The association between imaging features of TSCT and the expression of PD-L1 in patients with surgical resection of lung adenocarcinoma. *Clin Lung Cancer* 2019;20:e195-e207
15. Takada K, Toyokawa G, Okamoto T, Shimokawa M, Kozuma Y, Matsubara T, et al. A comprehensive analysis of programmed cell death ligand-1 expression with the clone SP142 antibody in non-small-cell lung cancer patients. *Clin Lung Cancer* 2017;18:572-582.e1
16. Sacher AG, Gandhi L. Biomarkers for the clinical use of PD-1/PD-L1 inhibitors in non–small-cell lung cancer: a review. *JAMA Oncol* 2016;2:1217-1222
17. Takada K, Okamoto T, Shoji F, Shimokawa M, Akamine T, Takamori S, et al. Clinical significance of PD-L1 protein expression in surgically resected primary lung adenocarcinoma. *J Thorac Oncol* 2016;11:1879-1890
18. Pan Y, Zheng D, Li Y, Cai X, Zheng Z, Jin Y, et al. Unique distribution of programmed death ligand 1 (PD-L1) expression in East Asian non-small cell lung cancer. *J Thorac Dis* 2017;9:2579-2586
19. Shukuya T, Carbone DP. Predictive markers for the efficacy of anti-PD-1/PD-L1 antibodies in lung cancer. *J Thorac Oncol* 2016;11:976-988
20. Fernandez-Bussy S, Pires Y, Labarca G, Vial MR. PD-L1 expression in a non-small cell lung cancer specimen obtained by EBUS-TBNA. *Arch Bronconeumol (Engl Ed)* 2018;54:290-292
21. Chen YB, Mu CY, Huang JA. Clinical significance of programmed death-1 ligand-1 expression in patients with non-small cell lung cancer: a 5-year-follow-up study. *Tumori* 2012;98:751-755
22. Toyokawa G, Takada K, Okamoto T, Kawanami S, Kozuma Y, Matsubara T, et al. Relevance between programmed death ligand 1 and radiologic invasiveness in pathologic stage I lung adenocarcinoma. *Ann Thorac Surg* 2017;103:1750-1757
23. Rizzo S, Petrella F, Buscarino V, De Maria F, Raimondi S, Barberis M, et al. CT radiogenomic characterization of EGFR, K-RAS, and ALK mutations in non-small cell lung cancer. *Eur Radiol* 2016;26:32-42
24. Liu Y, Kim J, Qu F, Liu S, Wang H, Balagurunathan Y, et al. CT features associated with epidermal growth factor receptor mutation status in patients with lung adenocarcinoma. *Radiology* 2016;280:271-280
25. Goldstraw P, Chansky K, Crowley J, Rami-Porta R, Asamura H, Eberhardt WE, et al. The IASLC lung cancer staging project: proposals for revision of the TNM stage groupings in the forthcoming (eighth) edition of the TNM classification for lung cancer. *J Thorac Oncol* 2016;11:39-51
26. Herbst RS, Soria JC, Kowanetz M, Fine GD, Hamid O, Gordon MS, et al. Predictive correlates of response to the anti-PD-L1 antibody MPDL3280A in cancer patients. *Nature* 2014;515:563-567
27. Sholl L. Molecular diagnostics of lung cancer in the clinic. *Transl Lung Cancer Res* 2017;6:560-569
28. Kim H, Chung JH. PD-L1 testing in non-small cell lung cancer: past, present, and future. *J Pathol Transl Med* 2019;53:199-206
29. Yu H, Boyle TA, Zhou C, Rimm DL, Hirsch FR. PD-L1 expression in lung cancer. *J Thorac Oncol* 2016;11:964-975
30. Zhang M, Li G, Wang Y, Wang Y, Zhao S, Haihong P, et al. PD-L1 expression in lung cancer and its correlation with driver mutations: a meta-analysis. *Sci Rep* 2017;7:10255
31. Firth D. Bias reduction of maximum likelihood estimates. *Biometrika* 1993;80:27-38
32. Heinze G, Schemper M. A solution to the problem of separation in logistic regression. *Stat Med* 2002;21:2409-2419
33. Akaike H. *Information theory and an extension of the maximum likelihood principle.* In Parzen E, Tanabe K, Kitagawa G, eds. *Selected papers of Hirotugu Akaike.* New York: Springer 1998:199-213
34. Hastie TJ, Pregibon D. *Chapter 6: generalized linear models.* In Hastie TJ, ed. *Statistical models in S.* 1st ed. New York: Taylor & Francis 1992:195-248
35. Venables WN, Ripley BD. *Modern applied statistics with S.* 4th ed. New York: Springer 2002:498

JOURNAL of
THE KOREAN SOCIETY of
RADIOLOGY

편평세포폐암에서 CT 영상 소견을 이용한 PD-L1 발현 예측

여성희[1] · 윤현정[1*] · 김인중[1] · 김여진[1] · 이 영[2] · 차윤기[3] · 박소현[4]

목적 CT 영상 소견을 이용하여 편평세포폐암에서 programmed death ligand 1 (이하 PD-L1)의 발현을 예측하는 모델을 구축해 보고자 하였다.

대상과 방법 PD-L1 발현검사 결과를 포함하고 있는 97명의 편평세포폐암 환자를 포함하였고 종양 치료 전 시행한 CT 영상 소견을 분석하였다. 전체 환자군과 40명의 진행성(≥ stage IIIB) 병기 환자군에 대하여 PD-L1 발현 예측을 위한 다중 로지스틱 회귀 분석 모델 구축을 시행하였다. 각각의 환자군에 대하여 곡선 아래 면적(areas under the receiver operating characteristic curves; 이하 AUCs)을 분석하여 예측력을 평가하였다.

결과 전체 환자군에서 '전체 유의인자 모델'(종양병기, 종양크기, 흉막결절, 폐전이)의 AUC 값은 0.652이며, '선택 유의인자 모델'(흉막결절)은 0.556이었다. 진행성 병기 환자군에서 '선택 유의인자 모델'(종양크기, 흉막결절, 폐소수전이, 간질성폐렴의 부재)의 AUC 값은 0.897이었다. 이러한 인자들 중 흉막결절과 폐소수전이는 높은 오즈비를 보였다(각각, 8.78과 16.35).

결론 본 연구에서의 모델은 편평세포폐암의 PD-L1 발현예측의 가능성을 보여주었으며 흉막결절과 폐소수전이는 PD-L1 발현을 예측하는데 중요한 CT 예측인자였다.

[1]중앙보훈병원 영상의학과,
[2]중앙보훈병원 보훈의학연구소,
[3]성균관대학교 의과대학 삼성서울병원 영상의학과,
[4]울산대학교 의과대학 서울아산병원 영상의학과